2,4-Diaminopyrimidine MK2 inhibitors. Part II: Structure-based inhibitor optimization

Christopher M. Harris, Anna M. Ericsson, Maria A. Argiriadi, Claude Barberis [†], David W. Borhani [‡], Andrew Burchat, David J. Calderwood, George A. Cunha, Richard W. Dixon [§], Kristine E. Frank, Eric F. Johnson [¶], Joanne Kamens [¶¶], Silvia Kwak, Biqin Li, Kelly D. Mullen, Denise C. Perron, Lu Wang, Neil Wishart, Xiaoyun Wu [‖], Xiaolei Zhang [††], Tami R. Zmetra [‡‡], Robert V. Talanian [*]

Abbott Laboratories, 100 Research Drive, Worcester, MA 01605-5314, USA

A B S T R A C T

We describe structure-based optimization of a series of novel 2,4-diaminopyrimidine MK2 inhibitors. Co-crystal structures (see accompanying Letter) demonstrated a unique inhibitor binding mode. Resulting inhibitors had IC_{50} values as low as 19 nM and moderate selectivity against a kinase panel. Compounds **15**, **31a**, and **31b** inhibit TNFα production in peripheral human monocytes.

© 2009 Elsevier Ltd. All rights reserved.

Tumor necrosis factor-α (TNFα) is an important target for biological drugs that are efficacious in rheumatoid arthritis (RA) and related autoimmune diseases.[1] The Ser/Thr kinase MK2 is required for TNFα production in an animal model of arthritis.[2] Although inhibitors of MK2 have been reported, none to our knowledge have progressed to clinical studies.[3–5]

In Part I[6], we described new in vitro tools to characterize MK2 inhibitors and enable structure-based drug design. We presented crystal structures that show an unexpected binding mode for 2,4-diaminopyrimidine inhibitors in the MK2 ATP binding site. The diaminopyrimidine ring was bound proximal to the DFG region, instead of adopting the commonly observed (for analogous inhibitors of other kinases) donor-acceptor mode of binding to the hinge region. This unexpected finding provided an opportunity to improve potency and possibly selectivity by optimizing compounds in several regions (Fig. 1): (1) substituents on the indazole ring to interact with the extended hinge region; (2) substituents on the pyrimidine-2-amine to access residues in the hydrophilic pocket and/or displace an ordered water behind gatekeeper residue
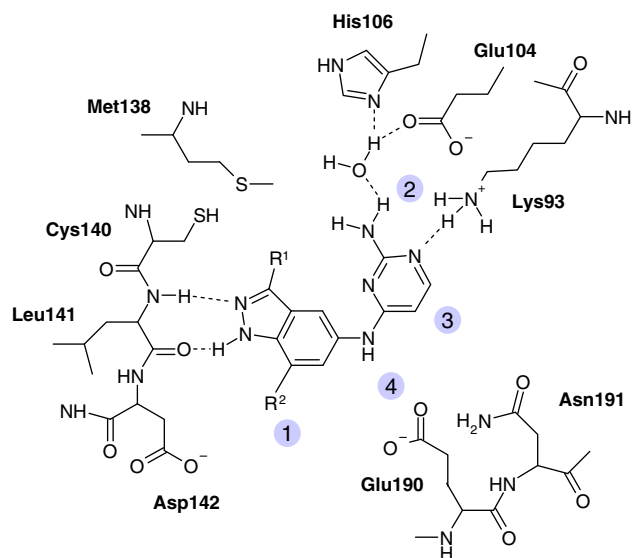

Figure 1. Structure-based optimization of compound **1**, $R^1 = R^2 = H$.

* Corresponding author. Tel.: +1 508 849 2581.
  E-mail address: bob.talanian@abbott.com (R.V. Talanian).
† Present address: Sanofi-Aventis, Bridgewater, NJ 08807, USA.
‡ Present address: DE Shaw Research, New York, NY 10036, USA.
§ Present address: Vertex Pharmaceuticals, Cambridge, MA 02139, USA.
¶ Present address: Abbott Laboratories, Abbott Park, IL 60064, USA.
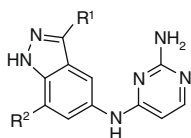¶¶ Present address: RXi Pharmaceuticals, Worcester, MA 01605, USA.
‖ Present address: Astra Zeneca, Waltham, MA 02451, USA.
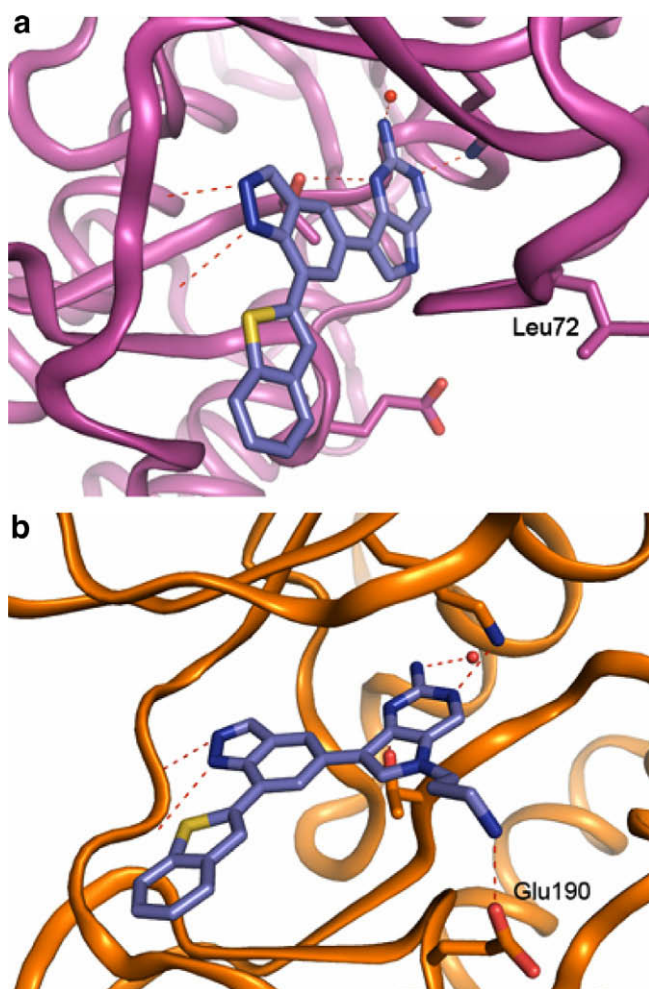†† Present address: Genzyme, Cambridge, MA 02142, USA.
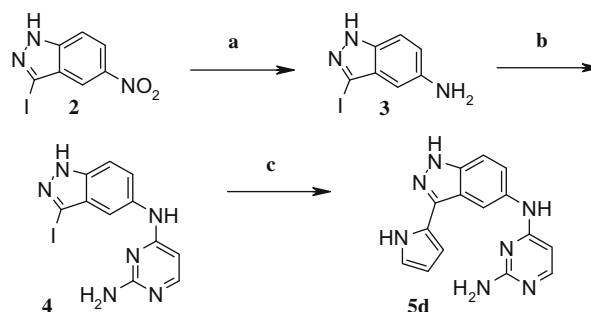‡‡ Present address: Agilux Laboratories, Worcester, MA 01605, USA.

Table 1
SAR at 3- and 7-positions of the indazole ring

Compound	R^1	R^2	MK2 IC$_{50}$ (µM)
1	H	H	24
4	I	H	14
5a	3-Thiophene	H	5.4
5b	2-Naphthalene	H	0.72
5c	2-Benzothiophene	H	1.6
5d	2-Pyrrole	H	1.3
10	H	I	9.1
11a	H	3-Thiophene	3.4
11b	H	2-Naphthalene	0.31
11c	H	2-Benzothiophene	0.16
11d	H	2-Benzofuran	0.16

Scheme 1. Reagents and conditions: (a) HI (57% stabilized), 90 °C, 2 h, 82%; (b) 2-amino-4-chloropyrimidine, EtOH, 80 °C, 2 h, 78%; (c) 1-(tert-butoxycarbonyl)pyrrole-2-boronic acid, NaHCO$_3$, DMF/H$_2$O, Pd(PPh$_3$)$_4$, 150 °C/µW, 15 min, 29%.
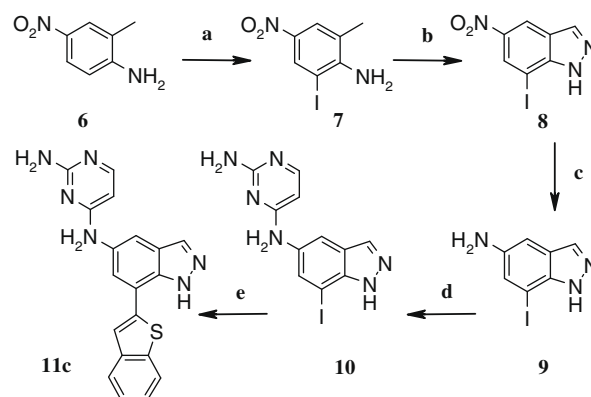
Scheme 2. Reagents and conditions: (a) IPy$_2$BF$_4$, CF$_3$SO$_3$H, DCM, 1 h, rt, 62%; (b) NaNO$_2$, AcOH/H$_2$O, 4 h, 60%; (c) Fe powder, AcOH, 80 °C, 6 h, 64%; (d) 2-amino-4-chloropyrimidine, EtOH, 80 °C, 2.5 h, 91%; (e) benzo[b]thiophene-2-boronic acid, Na$_2$CO$_3$, DME/H$_2$O, Pd(PPh$_3$)$_4$, 150 °C/µW, 10 min, 43%.

Figure 2. (a) Model of **15** (b) model of **31b** in MK2. Models were manually docked based on optimal hinge and Lys93 interactions.

Met138; (3) replacement of the pyrimidine ring with constrained bicyclic rings to reduce inhibitor conformational flexibility and to interact with the glycine rich loop; and (4) substitutions of the bridging nitrogen, or a similar position in a bicyclic system, to access ribose pocket residues.

Screening of the Abbott compound collection produced 4-(2-aminopyrimidin-4-ylamino) phenol, with an MK2[7] IC$_{50}$ of 34 µM. Concerns about in vivo liabilities of the phenol moiety led us to test bio-isosteres, resulting in compound **1**, which substitutes a 5-indazolyl group for the phenol (Table 1).

The binding mode (Fig. 1) suggested that 3- or 7-position substituents could make additional interactions with the MK2 extended hinge region (Tactic 1), requiring a 180° flip of the indazole moiety which preserves hinge interactions with Leu141 (Fig. 2a).[6] Representative routes to 3- and 7-substituted indazole analogs are described in Schemes 1 and 2, respectively. 3- or 7-iodo-substitutions had modest effects on inhibitor potency, whereas mono- or bicyclic aromatic groups at these positions gave significant gains (Table 1). 7-Position substitutions were slightly preferred. The 2-benzothiophene moiety, as in compound **11c**, was the optimal indazole 7-substitution and was retained in subse-
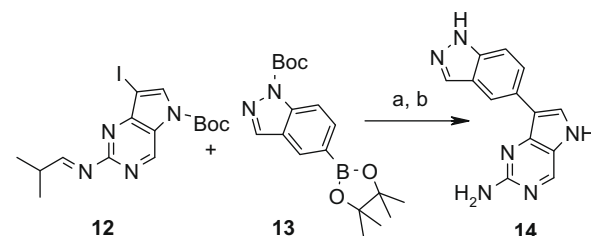
Scheme 3. Reagents and conditions: (a) Pd(PPh$_3$)$_4$, Cs$_2$CO$_3$, DME/H$_2$O, 60 °C, 24 h; (b) NaOH, EtOH, 100 °C, 2 h, 4% (two steps).
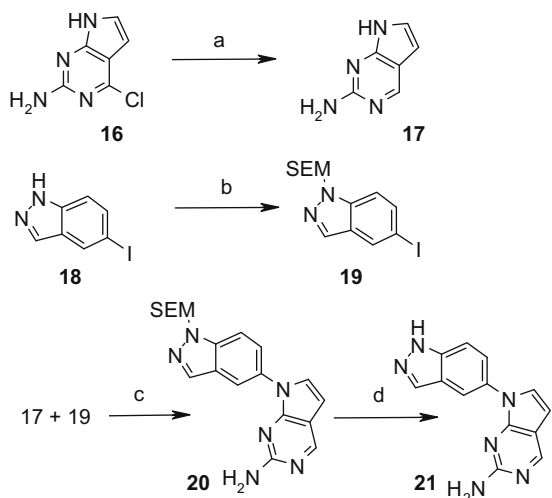
Scheme 4. Reagents and conditions: (a) 1 atm H₂/Pd–C/MeOH, 16 h, 81%; (b) SEM-Cl, TBABr, KOH, DCM, H₂O, 0 °C, 30 min, quant; (c) CuI, L-proline, K₂CO₃, DMSO, 90 °C, 16 h, 80%; (d) TBAF, ethylenediamine, THF, 50 °C, 16 h, 23%.

Table 2
Constrained A/B ring systems

Compound	X	Y	R	MK2 IC$_{50}$ (μM)
14	C	NH	5-Indazole	1.4
15	C	NH	7-(2-Benzothiophene)-5-Indazole	0.056
21	N	CH	5-Indazole	49
30	C	NCH₃	5-Indazole	1.9

In many protein kinases, a 'gatekeeper' residue blocks access to a hydrophobic pocket, occupancy of which has improved potency and selectivity for some inhibitors.[8] Our MK2 crystal structures[6] revealed that the hydrophilic pocket beyond Met108 contains solvent molecules (Fig. 1, Tactic 2). We attempted to occupy this space by substituting the exocyclic amine with a series of aromatic or aliphatic amides. All of these were inactive against MK2 (not shown).

To reduce conformational flexibility between the pyrimidine and indazole rings (Fig. 1, Tactic 3), the bridging nitrogen was constrained as a bicyclic system (Schemes 3 and 4). The pyrrolo[3,2-d]pyrimidine template of **14** gave a significant improvement in potency relative to the unconstrained pyrimidine **1** (Tables 1 and 2), with a small increase in molecular weight. Appending 7-(2-benzothiophene)-5-indazole onto the bicyclic template (**15**, Fig. 2a) resulted in potency gains similar to those obtained in the diaminopyrimidine scaffold. In contrast, the isomeric pyrrolo[2,3-d]pyrimidine template in **21** decreased potency. Methylation of the pyrrole N of **15** lead to the similarly active analog **30** indicating this might be a suitable position for further exploration.

Structural analyses[6] suggest that ribose pocket residues Glu145 and Glu190 can be accessed from the pyrrole NH of the pyrrolo[3,2-d]pyrimidines (Figs. 1 and 2, Tactic 4). Such molecules were synthesized according to Scheme 5. Only modest improvements in enzymatic potency were achieved (ethylamino **31a**, propylamino **31b**, or propionic acid **31h** substituents (Table 3)). In contrast to the binding mode of **15**, a model of **31b** (Fig. 2a and b) shows preference for an inactive form of MK2 (glycine rich loop rotated up) promoted by the pyrrole alkyl substitution. This may clash with the glycine rich loop. The terminal amine can form a salt bridge with Glu190. An analogous interaction was confirmed by an MK2 co-crystal structure with an alternate chemotype (not shown).

Our most potent MK2 inhibitor, **31a** (Table 3), was tested in a panel of 79 protein kinases. Compound **31a** was 2–10-fold more active against MK2 than eight other kinases (CHK2, PDK1, PKA, PKCζ, IKK-1, EMK, CDK2, and GSK3α), between 10- and 100-fold selective towards 22 kinases, and >100-fold selective toward 49 kinases (see Supplementary Table 1).

Several 5-substituted pyrrolo[3,2-d]pyrimidines inhibited lipopolysaccharide (LPS)-stimulated TNFα production in peripheral human monocytes (PHM) (Table 3). Compound **31b** had an IC$_{50}$

quent improvements of the series. Aliphatic groups at the benzothiophene ring 5-position gave modest potency improvements at the expense of a significant increase in molecular weight and so were not pursued further (not shown).
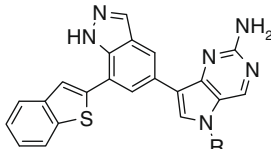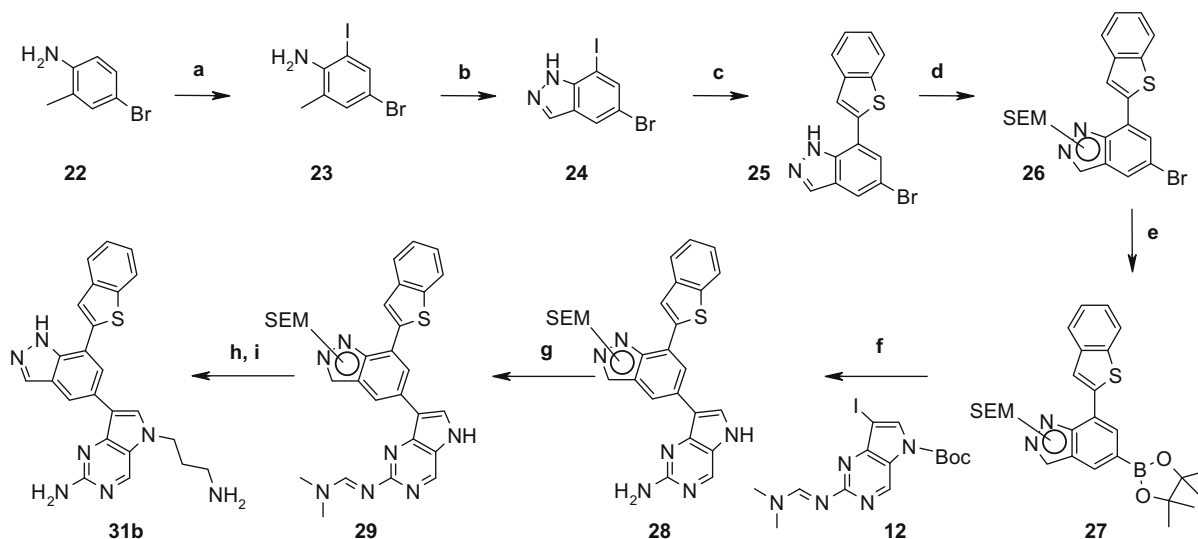
Scheme 5. Reagents and conditions: (a) Py₂IBF₄, DCM, 1.5 h, 77%; (b) NaNO₂, AcOH/H₂O, 15 min, 95%; (c) benzo[b]thiophene-2-boronic acid, Na₂CO₃, Pd(PPh₃)₄, DME/H₂O, 90 °C, 15 h, 70%; (d) t-BuOK, SEM-Cl, DMF, 100 °C, 18 h, 62%; (e) bis(pinacolato)-diboron, KOAc, Pd(dppf)Cl₂, 80 °C, 2.5 h, 39%; (f) **12**, Cs₂CO₃, Pd(PPh₃)₄, DME/H₂O, 65 °C, 16 h; NaOH/H₂O, 65 °C, 1 h, 60%; (g) 10 equiv DMF-DMA, CH₂Cl₂/CHCl₃, 45 °C, 16 h, 73%; (h) BocNH(CH₂)₃Br, NaH, DMF, 0 °C to rt, 16 h; (i) HCl, MeOH, 70 °C, 16 h, 10% (two steps).

Table 3
Ribose pocket

Compound	R	MK2 IC$_{50}$ (μM)	PHM TNFα IC$_{50}$ (μM)	PHM MTT TC$_{50}$ (μM)
15	H	0.056	0.055	>25
31a	$(CH_2)_2NH_2$	0.019	0.28	20
31b	$(CH_2)_3NH_2$	0.035	0.086	9.7
31c	$(CH_2)_4NH_2$	0.26		
31d	$(CH_2)_2$-4-Piperidine	0.96		
31e	$(CH_2)_3OH$	0.037		
31f	$(CH_2)_3OCH_3$	0.82		
31g	CH_2CO_2H	1.9	>25	>25
31h	$(CH_2)_2CO_2H$	0.02	>25	>25
31i	$(CH_2)_2CONH_2$	0.041		
31j	c-C_5H_6	>50		
31k	i-C_3H_7	0.49	1.0	>25
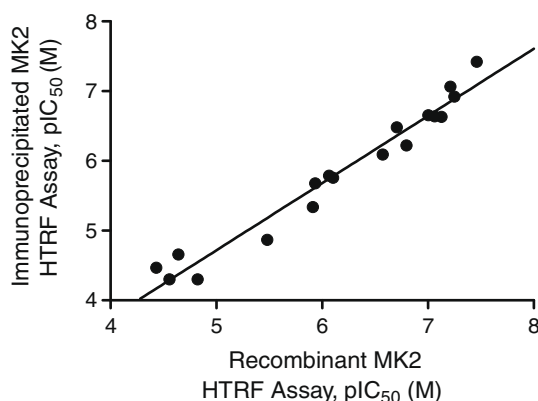
Figure 3. MK2 immunoprecipitated from human macrophages and recombinant MK2 exhibit similar inhibition behavior. Fit is a linear regression with slope = 0.96, y_{int} = −0.10, and r^2 = 0.96.

of 0.086 μM. This was substantially lower than that of phosphorylation of the MK2 substrate Hsp27 in the same cell (2.4 μM) and than the enzyme IC$_{50}$ (2.1 μM) obtained at 1 mM ATP (presumably closer to the cellular ATP concentration). Several inhibitors displayed toxicity determined using a 3-(4,5-dimethylthiazol-2-yl)-2,5-diphenyltetrazolium bromide assay, preventing meaningful PHM assay data interpretation (not shown).

Cellular potencies for **15** and **31b** were greater than predicted by enzymatic data at 10 μM ATP (Table 3), suggesting differences between recombinant MK2 and that in cells. Others have also observed poor correlations between inhibition of recombinant MK2 enzyme and cell potency.[2–4] We immunoprecipitated MK2 from monocytes[9] and showed that our compounds inhibited this material like recombinant enzyme (Fig. 3). We conclude that recombinant MK2 is not unlike MK2 in cells. We speculate that poor enzyme to cell correlations are due to other factors such as poor membrane penetration, inhibition of other targets that impact the cellular readout, or altered properties of MK2 in cells when in complex with other proteins.

In Sprague-Dawley rats, inhibitor **31b** had no oral bioavailability following a 10 mg/kg dose. A 3 mg/kg iv dose of **31b** gave $t_{1/2}$ = 5.5 h, V_{β} = 4 L/kg, AUC = 4.2 μg h mL^{-1}, and CL = 1.7 L h^{-1} kg^{-1}. We discontinued development of this series due to our difficulty in further improving enzymatic potency, cellular potency, and in achieving significant oral exposure.

Supplementary data

Supplementary data associated with this article can be found, in the online version, at doi:10.1016/j.bmcl.2009.10.103.

References and notes

1. Gabay, C. *Exp. Opin. Biol. Ther.* **2002**, *2*, 135.
2. Gaestel, M.; Kotlyarov, A.; Kracht, M. *Nat. Rev. Drug Disc.* **2009**, *8*, 480.
3. Anderson, D. R.; Meyers, M. J.; Vernier, W. F.; Mahoney, M. W.; Kurumbail, R. B.; Caspers, N.; Poda, G. I.; Schindler, J. F.; Reitz, D. B.; Mourey, R. J. *J. Med. Chem.* **2007**, *50*, 2647.
4. Wu, J.-P.; Wang, J.; Abeywardane, A.; Andersen, D.; Emmanuel, M.; Gautschi, E.; Goldberg, D. R.; Kashern, M. A.; Lukas, S.; Mao, W.; Martin, L.; Morwick, T.; Moss, N.; Pargellis, C.; Patel, U. R.; Patnaude, L.; Peet, G. W.; Skow, D.; Show, R. J.; Ward, Y.; Werneburg, B.; White, A. *Bioorg. Med. Chem. Lett.* **2007**, *17*, 4664.
5. Schlapbach, A.; Feifel, R.; Hawtin, S.; Heng, R.; Koch, G.; Moebitz, H.; Revesz, L.; Scheufler, C.; Velcicky, J.; Waelchli, R.; Huppertz, C. *Bioorg. Med. Chem. Lett.* **2008**, *18*, 6142.
6. Argiriadi, M. A.; Ericsson, A. M.; Harris, C. M.; Banach, D. L.; Borhani, D. W.; Calderwood, D. J.; Demers, M. D.; DiMauro, J.; Dixon, R. W.; Hardman, J.; Kwak, S.; Li, B.; Mankovich, J. A.; Marcotte, D.; Mullen, K. D.; Ni, B.; Pietras, M.; Sadhukhan, R.; Sousa, S.; Tomlinson, M. J.; Wang, L.; Xiang, T.; Talanian, R. V. *Bioorg. Med. Chem. Lett.* 2009, doi:10.1016/j.bmcl.2009.10.102.
7. Argiriadi, M. A.; Sousa, S.; Banach, D.; Marcotte, D.; Xiang, T.; Tomlinson, M. J.; Demers, M.; Harris, C.; Kwak, S.; Hardman, J.; Pietras, M.; Quinn, L.; DiMauro, J.; Ni, B.; Mankovich, J.; Borhani, D. W.; Talanian, R. V.; Sadhukhan, R. *BMC Struct. Biol.* 2009, *9*, 16.
8. Okram, B.; Nagle, A.; Adrian, F. J.; Lee, C.; Ren, P.; Wang, X.; Sim, T.; Xie, Y.; Wang, X.; Xia, G.; Spraggon, G.; Warmuth, M.; Liu, Y.; Gray, N. S. *Chem. Biol.* **2006**, *13*, 779.
9. Monocytes were differentiated 5 days in RPMI with 50 ng/mL M-CSF then stimulated 30 min with 50 ng/mL LPS. After PBS washing, cells were lysed in 50 mM Tris pH 7.5, 150 mM NaCl, 1% Triton X-100, 1 mM EDTA, 1 mM EGTA, 20 mM NaF, 10 mM $Na_4P_2O_7$, 1 mM Na_3VO_4, and Roche protease cocktail 11836153001. MK2 was immunoprecipitated with anti-MK2 agarose (Millipore) and used in the HTRF MK2 assay.[7]